Physiol Genomics 39: 61–71, 2009.
First published July 14, 2009; doi:10.1152/physiolgenomics.00076.2009.

Transcriptional changes in right ventricular tissues are enriched in the outflow tract compared with the apex during chronic pulmonary embolism in rats

John Zagorski, Maria Obraztsova, Michael A. Gellar, Jeffrey A. Kline, and John A. Watts

Department of Emergency Medicine, James G. Cannon Research Center, Carolinas Medical Center, Charlotte, North Carolina

Submitted 1 May 2009; accepted in final form 13 July 2009

Zagorski J, Obraztsova M, Gellar MA, Kline JA, Watts JA. Transcriptional changes in right ventricular tissues are enriched in the outflow tract compared with the apex during chronic pulmonary embolism in rats. *Physiol Genomics* 39: 61–71, 2009. First published July 14, 2009; doi:10.1152/physiolgenomics.00076.2009.—Moderate to severe pulmonary embolism (PE) can cause pulmonary arterial hypertension and right ventricular (RV) heart damage. Previous studies from our laboratory indicate that the basal outflow tract of the RV is injured and has acute inflammation followed by tissue remodeling while the apex appears normal. The present studies examine transcription responses to chronic PE in RV apex and outflow tracts using DNA microarrays to identify transcription responses by region. Changes predominated in the RV outflow tract (8,575 genes showed ≥1.5-fold expression change). Gene ontology and KEGG analyses indicated a significant decrease in genes involved in cellular respiration and energy metabolism and increases in inflammatory cell adhesion molecules and extracellular matrix proteins. Signal pathways for wound healing such as fibroblast growth factor, collagen synthesis, and CCN proteins (named for the first three members of the family: cysteine-rich protein 61, connective tissue growth factor, and nephroblastoma overexpressed gene) were strongly upregulated. In comparison, few genes (422) showed significant change in the RV apex tissue. Apex-selective genes included two genes affecting metabolism and a stretch-sensitive transcription factor (ankyrin repeat domain 1). We conclude that the RV outflow tract is subject to strong proinflammatory and profibrotic remodeling transcriptional responses in chronic PE. Severe loss of genes involved in cellular respiration is consistent with previous histology indicating a shift in cell types present within the outflow tract tissue away from highly energy-dependant cardiomyocytes to less metabolically active cells during remodeling. The apex region of the RV had few compensating adaptations.

heart; pulmonary hypertension; inflammation; microarray; Wnt signaling

PULMONARY EMBOLISM (PE) occurs in ~600,000 patients each year in the US, leading to as many as 60,000 deaths (8, 9). Mortality rate exceeds 15% in the first 3 mo, but patient mortality and morbidity increase dramatically with the presence of right ventricular (RV) dysfunction (9, 19, 25, 27). Usually observed with echocardiography, the "McConnell sign" is a particular pattern of resultant injury with hypokinesis in the basal and mid free wall but normal motion in the apex of the RV that has been used in the diagnosis and management of significant PE in the clinical setting (9, 22), Reasons for the regional localization of injury within the RV and mechanisms of injury are not well defined. PE usually results from the formation of blood clots in the deep veins, which detach and flow into the pulmonary arterial system (28). The resultant occlusion increases pulmonary vascular resistance and causes pulmonary hypertension (PH), which subjects the right ventricle to increased work load, increased wall tension, and shear force and compression of the coronary vessels, leading to functional ischemic injury to cardiomyocytes (32). Myocyte lysis occurs and the myocardium converts to a proinflammatory phenotype in humans (1, 15, 16). The contributions of inflammation to the process of RV injury and remodeling are just beginning to be understood.

Much remains to be uncovered about the mechanisms of damage to heart and lung function. We established a rat model of irreversible PE to examine this pathology (5, 17, 34). The acute responses include pulmonary hypertension, increased right ventricular systolic pressure and RV contractile dysfunction. Acute PE also causes a severe inflammatory response in RV tissue that can be mitigated by treatment with nonsteroidal anti-inflammatory drugs (17), by neutrophil depletion using anti-rat neutrophil antiserum (31), or by treatment with an antibody against the CXC chemokine CINC-1 (CXCL1) (35). These three anti-inflammatory treatments also improve RV function following PE, suggesting one approach to reducing cardiac damage during PE.

Our original screen for proinflammatory genes was specifically targeted at a select subset of chemokines using a single gene approach in the 18 h model of PE (31). This was subsequently expanded to assess the time course of genome-wide transcriptional regulation in RV tissue during acute PE (2, 6, and 18 h) using DNA microarrays (36). The data indicated that few genes changed 2 h after inducing PE (76 genes ≥1.5-fold changed vs. controls). Later in PE (18 h), when cardiac damage can be detected, nearly 6,000 genes were altered in expression relative to controls (31). Gene Ontology (GO) and KEGG (Kyoto Encyclopedia of Genes and Genomes) pathway analyses showed a large number of proinflammatory genes expressed and a shift in metabolic pathways from an adult to a fetal gene program (e.g., fatty acid metabolism downregulated).

The PE model was recently extended to examine changes over 6 wk (chronic PE). Changes were concentrated in the basal outflow region of the RV, which developed an almost transparent appearance. Histological evaluation showed the depletion of myocyte content, the presence of myofibroblasts, neovessel formation, collagen deposition, and persistence of $CD68^+$ monocytes selectively within the outflow tract (29). Thus, the outflow tract appeared to be converting to fibrotic scar tissue. In contrast, the apex tissue from chronic PE hearts had a normal appearance and histology. Transcriptional changes have not previously been examined in this chronic

Address for reprint requests and other correspondence: J. A. Watts, Dept. of Emergency Medicine, Carolinas Medical Center, James G. Cannon Research Center, 1542 Garden Terrace, Rm. 302, Charlotte, NC 28203 (e-mail: jwatts@carolinas.org).

model of PE. The present studies examine transcriptional changes in the RV apex and outflow regions during chronic PE using DNA microarrays. The data complement our previous genomic evaluation of changes during acute PE (36) and the previous pathological and histological description of chronic PE (29) and also reveal a large disparity in quantitative gene expression between the RV outflow tract and RV apex.

MATERIALS AND METHODS

Animal treatments and induction of PE. Experiments were performed using male Sprague-Dawley rats (375–400 g). All experiments were conducted in accordance with the *Guide for the Care and Use of Laboratory Animals* and were approved by the Institutional Animal Care and Use Committee of the Carolinas Medical Center. Prior to use, rats had ad libitum access to food and water.

PE was induced in anesthetized rats by intrajugular vein injection of polystyrene microsphere beads [mean diameter 25 ± 1 μm, #7525A; Microgenics, Fremont, CA (formerly Duke Scientific, Palo Alto, CA); 2.0 million beads/100 g body wt] and vehicle-treated animals received surgery and vehicle injection as previously described (5, 17, 31, 34). Six weeks later, hearts were surgically removed from anesthetized rats by midline thoracotomy and perfused briefly by the Langendorff technique with Krebs-Henseleit bicarbonate buffer to remove blood. RVs were separated and further dissected into basal outflow tract and apical sections. Tissues were quick-frozen with liquid nitrogen-cooled Wollenberger clamps and then stored at −70°C. Thus, there were two experimental groups (vehicle and PE); each consisting of five rats and the outflow tract and apex tissues of each group were analyzed separately.

Sample processing. Frozen RV apex and base samples were pulverized with a custom-built stainless steel mortar and pestle chilled with liquid nitrogen. Approximately 25–50 mg of tissue powder was then processed into RNA by the TRIzol method (Invitrogen). The extracted RNAs were purified on Qiagen RNeasy columns and 5 μg total RNA was converted to double-stranded cDNA with a Superscript double-stranded cDNA synthesis kit (Invitrogen). The cDNA was then processed, spiked with bioB, bioC, bioD, and cre hybridization controls, and the fragmented cRNAs were hybridized to Affymetrix Rat Genome 230 v2.0 microarrays according to Affymetrix procedures. Each array was scanned twice by an Agilent Gene Array Scanner G2500A (Agilent Technologies, Palo Alto, CA).

Data analysis. Microarray data were analyzed with GeneSifter web-based software (Geospiza, Seattle, WA). Affymetrix ".cel" files were up-loaded to the GeneSifter web site using GC-RMA normalization into "Pair-wise" and "Project" folders for access to *t*-test and ANOVA statistical methods, respectively. Each analysis was conducted with Benjamini and Hochberg adjustment for false discovery. Sample clustering analysis was done with the GeneSifter CLARA function (Clustering of Large Applications) using unfiltered microar-

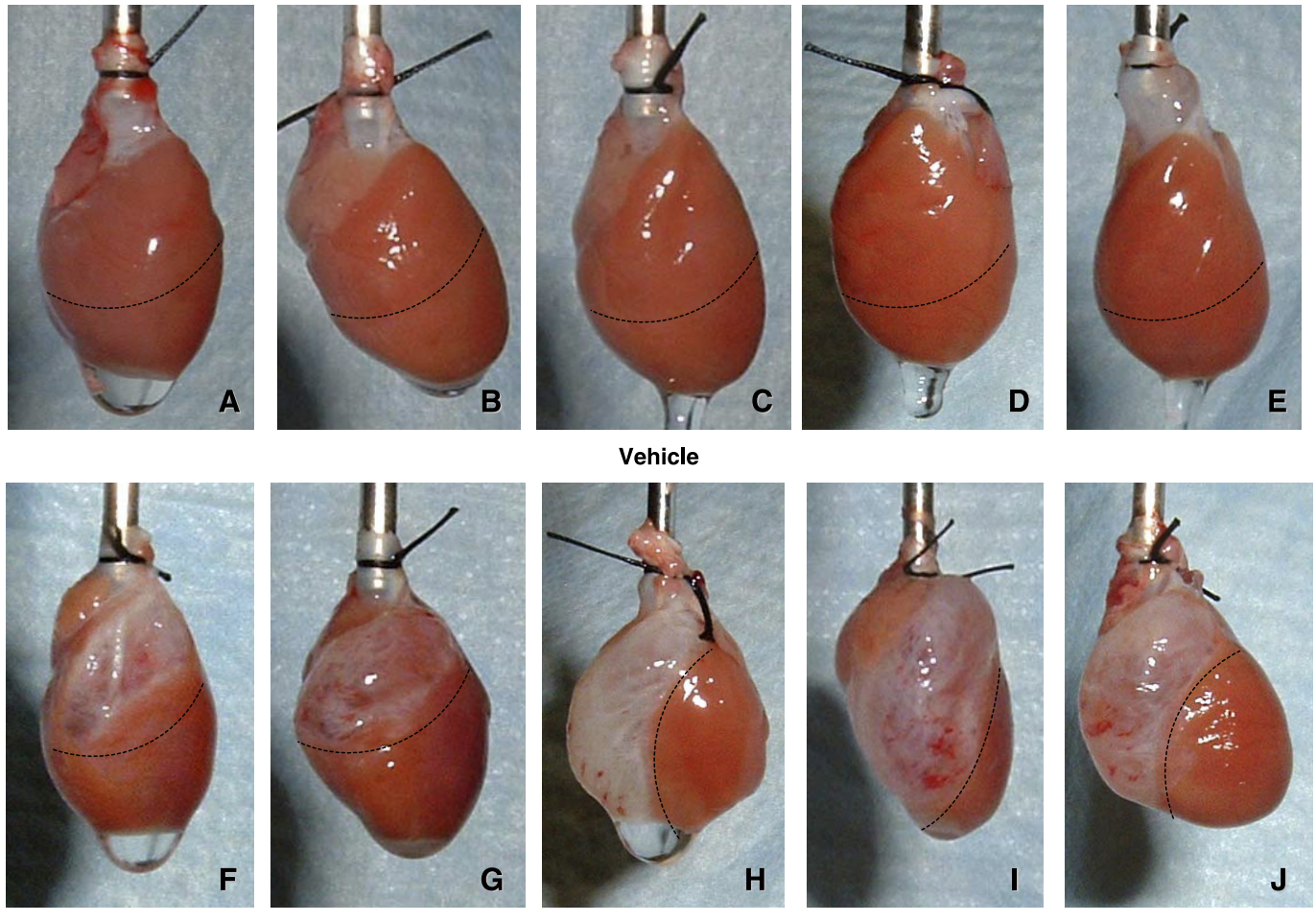

Fig. 1. Photographs of hearts used in the study: vehicle (*A–E*), pulmonary embolism (PE, *F–J*). Hearts were photographed while suspended from the Langendorff perfusion cannula in a position with the right ventricles (RV) facing the camera. The approximate demarcations between regions of the RV sectioned into outflow tracts and apexes are indicated with dashed lines [outflow tracts are above the lines (O), apexes are below the lines (A)].

ray data. Comparison of the four groups was done using an ANOVA. Pair-wise analyses of expression ratios for the four possible group comparisons were done using *t*-tests. The Pattern Analysis function was used to identify genes selectively altered in the PE apex group. Sample groups were compared using ANOVA, followed by Tukey's test. Only genes with known probe sets are included in tables. Genes with unspecified transcribed loci or with speculative function or ontological annotations are not shown.

Gene expression comparisons between the sample groups were organized into KEGG and GO reports, which were screened for potential biological significance based on their z-scores, with z-scores of $\geq +2.0$ or ≤ -2.0 being used as the cut-off for divergence from chance. ANOVA, pair-wise comparisons, GO analyses, and KEGG pathway reports were done using annotations current in the 8/22/08 update of GeneSifter, except for the expanded lists in Supplement 6 (Biological Process - biological adhesion; Cellular Compartment - envelope and extracellular region part), which were derived from the 1/26/09 GeneSifter update.[1] Some gene annotations and GO/KEGG assignments may have changed during the preparation and submission of this manuscript. All microarray data have been deposited in the NIH/NCBI "GEO" database (http://www.ncbi.nlm.nih.gov/projects/geo; GEO accession number GSE11851).

Validation of microarray results with quantitative real-time RT-PCR. Our previous studies demonstrate an extremely high correlation between fold change detected in the microarray platform and real-time PCR techniques (36). This was again confirmed in the present studies using six genes that represent a range of gene expression ratios presented in the PE outflow vs. vehicle outflow comparison (data not shown).

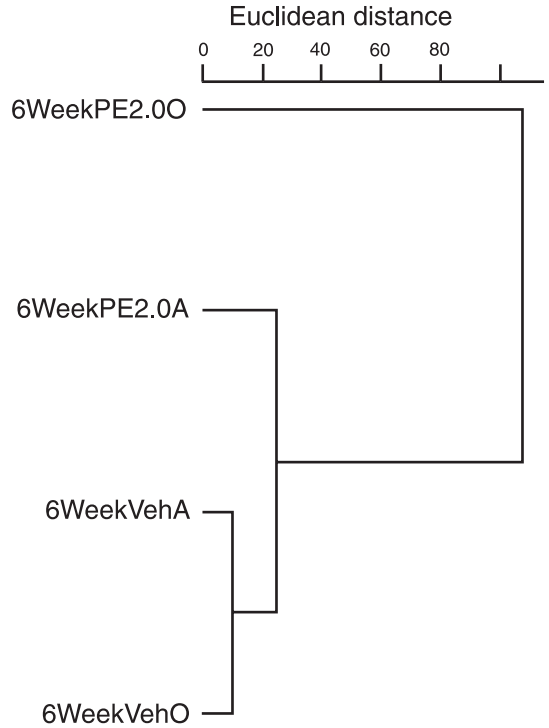

Fig. 2. Hierarchical clustering of 4-group ANOVA results using 2-fold expression change threshold. The scale at the top of the figure represents relative Euclidean distance between sample groups.

RESULTS

Gross anatomy of rat hearts after 6 wk of PE. Exterior views of the five PE rat hearts and five vehicle controls used for this study are shown in Fig. 1. Hearts were positioned to show RVs. Left ventricles are positioned behind the RVs in these pictures and are not clearly visible. The approximate delineations of the RV bases and apexes used for surgical separation prior to sample preparation are shown in each panel with dashed lines. Compared with the vehicle-treated hearts, the outflow tracts of the PE heart RVs are translucent in appearance, while the apex tissues appear similar to the apexes of the vehicle control.

Distribution of microarray data into expression clusters. The base and apex regions of five control and five PE hearts were compared by microarray analysis. Overall divergence between the sample groups was assessed with the CLARA function of GeneSifter, using unfiltered microarray expression data that was constrained to associate into four clusters. Two basic patterns of expression were observed: PE outflow $>$ PE apex $>$ both vehicle groups; PE outflow $<$ PE apex $<$ vehicles (not shown), indicating that the outflow tract samples had greater alteration in gene expression than did the PE apex samples, relative to the two vehicle groups.

Comparison of PE samples with vehicle samples using expression thresholds and ANOVA. The four treatment groups were compared by ANOVA using the vehicle apex samples as the control group. Expression thresholds were set at 1.5-, 2.0-, or 5.0-fold. A total of 8,575 genes met the search parameters when the threshold was set for 1.5, while 4,591 genes met the 2-fold threshold, and 453 genes met the 5-fold threshold. The ANOVA results from the 2-fold threshold were then subjected to hierarchical clustering, resulting in the relationships shown in Fig. 2. The two control groups clustered closely together while the PE outflow group was separated by a large relative Euclidean distance on the horizontal axis. Consistent with the CLARA data, the PE apex group was closer in distance to the controls than the PE outflow group. A spreadsheet containing the complete exported data file from the ANOVA comparison with the 2-fold expression threshold is available in Supplement 1.

HEAT maps established with 1.5-, 2-, and 5-fold threshold ANOVA were too extensive to present. A "zoom-able" JPEG version of the 5-fold threshold ANOVA is available as a HEAT map in Supplement 2. Changes in gene expression were enriched in the PE outflow group. Most genes showed increased expression relative to apex vehicles (370 of 453 significant genes with 5-fold expression change) while 81 had decreased expression. Portions of the 5-fold ANOVA were assembled into the collage shown in Fig. 3, showing the top 20 most variant genes with increased expression (red), bottom 20 most variant genes with decreased expression (green), and 15 genes that are present at the juncture of red-green transition relative to the vehicle apex.

Thus, CLARA, hierarchical clustering, and ANOVA comparisons indicated that the PE outflow tract was the primary site of transcriptional changes following 6 wk of PE, and the PE apex was relatively quiet in comparison. Furthermore, genes with increased expression greatly outnumbered genes with decreased expression. These data led to pair-wise comparisons of the PE outflow tract and apex sample group with their corresponding vehicle groups for further analyses.

Pair-wise ratios of gene expression, PE versus vehicle. Four sample groups were compared using *t*-tests as follows: vehicle outflow vs. vehicle apex; PE outflow vs. PE apex; PE outflow

[1] The online version of this article contains supplemental material.

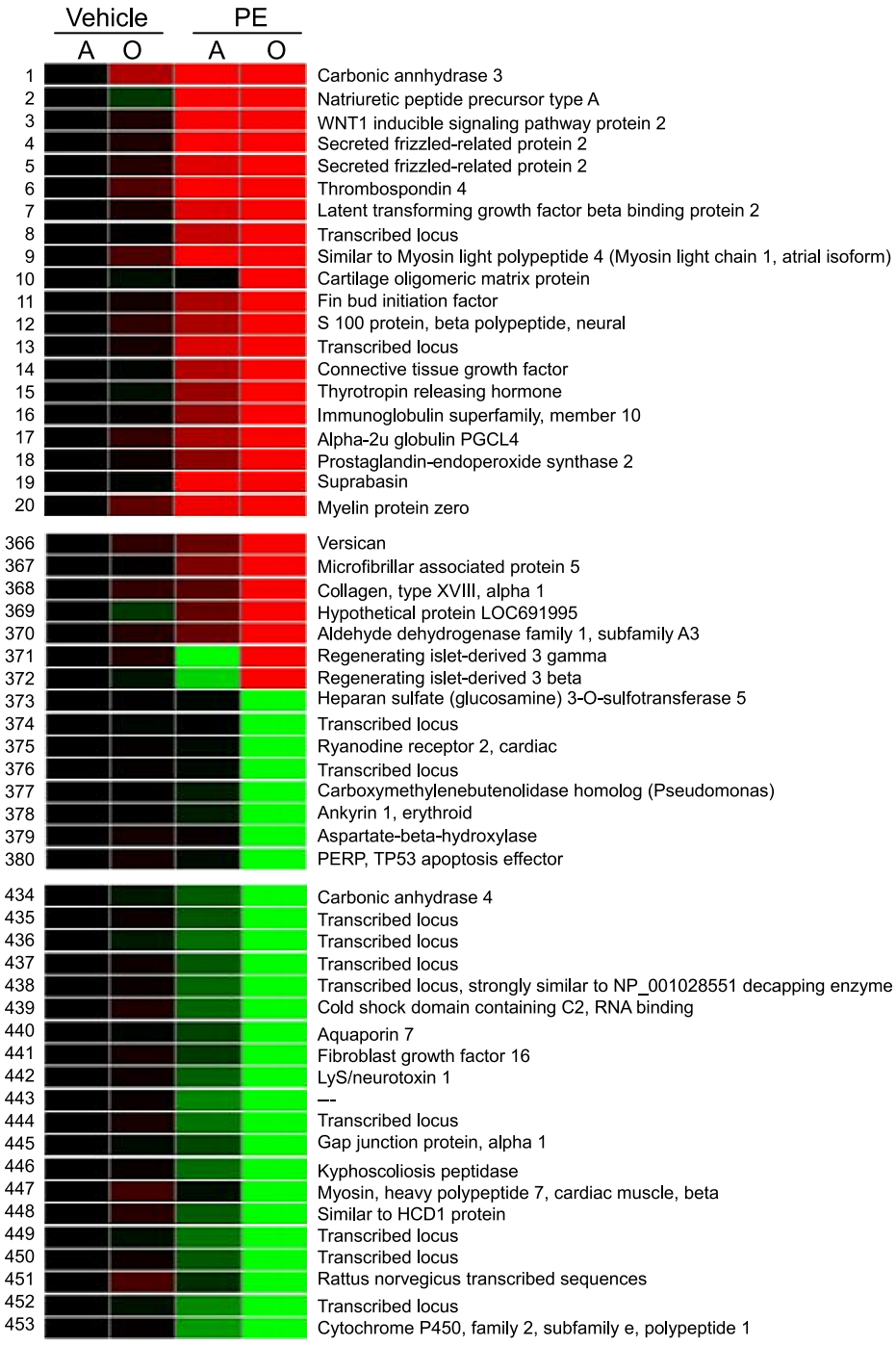

Fig. 3. HEAT map of ANOVA results using a 5-fold expression threshold. A collage of 3 sections of the HEAT map showing the top 20 "red" genes, bottom 20 "green" genes, and 15 genes at the red-green boundary is presented. Red color indicates increased expression relative to control while green represents decreased expression. *Lane 1*, vehicle apex (A); *lane 2*, vehicle outflow tract (O); *lane 3*, PE apex (A); *lane 4*, PE outflow tract (O).

vs. vehicle outflow; PE apex vs. vehicle apex. These data are summarized in Table 1; 8,575 genes were altered in expression by ≥1.5-fold in the PE outflow vs. vehicle outflow comparison. Almost half of these had expression ratios between 1.5- and 2-fold, and >94% were under 5-fold, but 90 genes had expression ratios of ≥10-fold. Similar changes were observed in the PE outflow and PE apex comparison. As seen in the ANOVA and clustering analyses, a much smaller transcriptional response was seen in the comparison of PE apex vs. vehicle apex.

The genes with the highest fold-changes in the PE outflow vs. vehicle outflow and PE apex vs. vehicle apex are shown in Tables 2 and 3. Note that genes common to both tables are highlighted in boldface. Complete lists of the genes identified in these tables are available in Supplements 3 and 4.

Apex-selective expression. We postulated that damage to the outflow tract might be compensated for with changes in the apex region. Therefore, two approaches were used to identify genes with an apex-selective response. Genes with high expression ratios in Table 3 (apex vs. apex) but not listed in Table 2 (outflow vs. outflow) were compiled in Table 4, resulting in a small group of genes that may represent apex-selective components of the PE pathophysiology. The GeneSifter Pattern Recognition function was also used to identify a defined cluster of genes with an apex-predominant expression by

Table 1. *Genes differentially expressed in the 4 pair-wise comparisons of PE2.0 and vehicle sample groups*

Ratio	Genes Altered, *n*
PE2.0 outflow tract/vehicle outflow tract	8,575 ≥1.5-fold
	4,591 ≥2.0-fold
	474 ≥5.0-fold
	90 ≥10.0-fold
	21 ≥20.0-fold
PE2.0 outflow tract/PE2.0 apex	7,293 ≥1.5-fold
	3,546 ≥2.0-fold
	201 ≥5.0-fold
	40 ≥10.0-fold
	7 ≥20.0-fold
PE2.0 apex/vehicle apex	422 ≥1.5-fold
	72 ≥2.0-fold
	5 ≥5.0-fold
	1 ≥10.0-fold
Vehicle outflow tract/vehicle apex	7 ≥1.5-fold
	0 ≥2.0-fold

Values represent gene expression ratios between the four groups and are independent of "sign" (± fold changes in expression included). The number of genes with altered expression is stratified by fold changes. PE, pulmonary embolism.

searching the ANOVA data from Supplement 1 for genes with the following expression pattern: vehicle apex group (control) = 1, PE apex > *n*, PE outflow < *n*, vehicle outflow < *n*, where *n* = fold-changes in mean gene expression relative to the vehicle apex control group. These data are shown in HEAT map format (Fig. 4) with threshold set at $n = 2$ (*top* panel) and at $n = 0.5$ (*bottom* panel). The complete list of genes identified by the pattern analyses is available in Supplement 5.

GO and KEGG pathway analyses of pair-wise comparisons: PE outflow vs. vehicle outflow. The altered genes identified in the PE outflow vs. vehicle outflow pair-wise comparison were sorted into ontologies and pathways by the GeneSifter GO and KEGG summary functions using the *t*-test (Supplement 3) for ratios ≥2.0. GO searches were done sequentially on the first hierarchy of GO terms, Biological Process, Cellular Components, and Molecular Functions. The results of sorting significantly altered genes in the outflow/outflow comparison into their primary GO terms (Biological, Cellular, and Molecular) are summarized in Table 5. Only GO terms with z-scores ≥+2.0 or ≤−2.0 in at least one expression ratio (▲ or ▼) were included in the table. Approximately half of all the secondary GO terms contained under the three primary terms met this z-score cut-off. Secondary terms with especially large z-scores are highlighted in italics and include developmental process, extracellular matrix changes, and biological adhesion, as well as several terms associated with energy utilization (catalytic activity, organelle, electron carrier activity). The individual genes in the spreadsheet in Supplement 3 that are annotated with these terms can be searched by standard Microsoft Excel methods.

A summary of KEGG pathways altered in the outflow/outflow comparison are listed in Table 6. Z-scores were again used for initial screening of pathways. Only pathways with at

Table 2. *Sample of genes altered in expression in the PE2.0 outflow vs. vehicle outflow comparison*

Ratio	Dir.	Adj. *P* Value	Gene Name	Gene ID
70.97	**up**	**3.49E-04**	**carbonic anhydrase 3**	**Car3**
70.64	**up**	**1.14E-04**	**WNT1 inducible signaling path. protein 2**	**Wisp2**
67	up	4.96E-04	cartilage oligomeric matrix protein	Comp
58.1	**up**	**3.56E-04**	**secreted frizzled-related protein 2**	**Sfrp2**
46.37	up	6.19E-05	retinol binding protein 4, plasma	Rbp4
45.46	**up**	**9.33E-05**	**natriuretic peptide precursor type A**	**Nppa**
38.65	**up**	**2.70E-05**	**latent TGF-β binding protein 2**	**Ltbp2**
32.35	up	5.43E-05	complement component 4, gene 2	C4a
29.92	up	1.26E-05	follistatin	Fst
27.28	up	1.75E-05	growth-associated protein 43	Gap43
22.41	up	1.26E-04	carboxypeptidase X 2 (M14 family)	Cpxm2
22.38	up	1.19E-04	neuronatin	Nnat
21.7	**up**	**8.28E-05**	**thrombospondin 4**	**—**
21.37	up	2.14E-04	adiponectin, C1Q and collagen domain cont.	Adipoq
21.2	up	3.70E-04	claudin 11	Cldn11
20.95	up	4.97E-04	actin, γ2, smooth muscle, enteric	Actg2
19.73	up	5.54E-05	glial fibrillary acidic protein	Gfap
19.57	**up**	**1.56E-04**	**fin bud initiation factor**	**Fibin**
19.49	up	1.03E-04	Thyrotropin-releasing hormone	Trh
19.39	**up**	**4.94E-05**	**S100 protein, β-polypeptide, neural**	**S100b**
19.24	up	1.77E-04	ceruloplasmin	Cp
18.68	up	1.36E-03	nephroblastoma overexpressed gene	Nov
18.38	up	1.00E-04	ceruloplasmin	Cp
18.18	up	8.00E-05	K^+-conductance Ca^{2+}-activated channel, Mα1	Kcnma1
18.13	up	2.49E-04	cell death-inducing DFFA-like effector c	Cidec
18.05	up	4.70E-04	transmembrane protein 178	Tmem178
17.53	**up**	**1.24E-04**	**connective tissue growth factor**	**Ctgf**
15.64	up	7.36E-04	thyroid hormone-responsive protein	Thrsp
15.46	up	2.20E-04	calponin 1	Cnn1
15.39	up	2.30E-04	Fc receptor-like S, scavenger receptor	Fcrls
15.28	up	2.79E-03	gremlin 1	Grem1

Ratios represent PE outflow/vehicle outflow expression. Out of the 4,591 genes with ratios ≥2.0, only genes with ratios >15 are included in this table. Adjusted *P* values are from *t*-tests with Benjamini and Hochberg corrections for false discovery. Genes common to this table and Table 3 are listed in boldface. The complete list of 4,591 genes is available in Supplement 1.

Table 3. *Sample of genes altered in expression in the PE2.0 apex vs. vehicle apex comparison*

Ratio	Dir.	Adj. *P* Value	Gene Name	Gene ID
20.39	**up**	**0.004511**	**natriuretic peptide precursor type A**	**Nppa**
7.36	**up**	**0.031542**	**carbonic anhydrase 3**	**Car3**
7.12	**up**	**0.007067**	**thrombospondin 4**	
6.4	**up**	**0.002462**	**WNT1 inducible signaling pathway protein 2**	**Wisp2**
5.82	up	0.003179	suprabasin	Sbsn
4.54	**up**	**0.005269**	**secreted frizzled-related protein 2**	**Sfrp2**
4	down	0.026277	regenerating islet-derived 3γ	Reg3 g
3.7	up	0.014745	myelin protein zero	Mpz
3.41	**up**	**0.004511**	**secreted frizzled-related protein 2**	**Sfrp2**
3.4	**up**	**0.004511**	**latent TGF-β binding protein 2**	**Ltbp2**
3.24	up	0.020919	similar to PIRA5	Lilrb3
3.15	up	0.005269	collagen, type VIII, α1	Col8a1
3.08	up	0.004511	natriuretic peptide precursor type B	Nppb
2.84	down	0.027423	angiopoietin-like 4	Angptl4
2.71	up	0.042615	hepcidin antimicrobial peptide	Hamp
2.69	up	0.005269	similar to Ig superfamily containing leu-rich repeat	LOC686539
2.65	**up**	**0.009598**	**connective tissue growth factor**	**Ctgf**
2.61	up	0.014465	similar to Coatomer γ-2 subunit (γ-2 coat protein)	RGD1566215
2.57	**up**	**0.002462**	**fin bud initiation factor**	**Fibin**
2.55	**up**	**0.011779**	**S100 protein, β-polypeptide, neural**	**S100b**
2.54	up	0.004579	nuclear localized factor 2	Nlf2
2.53	up	0.007562	monoamine oxidase A	
2.53	up	0.004511	peptidase inhibitor 16	Pi16
2.52	up	0.023001	α-2 μ globulin PGCL4	Obp3
2.51	up	0.004511	peptidase inhibitor 16	Pi16

Ratios represent PE2.0 expression/vehicle expression. Out of 422 genes with ratios ≥1.5, only genes with ratios >2.5 are included in the table. Adjusted *P* values are from *t*-tests with Benjamini and Hochberg corrections for false discovery. Genes common to this table and Table 2 are listed in boldface. The complete list of 422 genes is available in Supplement 2.

least one z-score >+2.0 were included in the table (. 29 listed out of 170 pathways in the 8/08 GeneSifter update). Examination of the KEGG pathways with large z-scores identified several pathways associated with cellular respiration, cell-cell, and cell-matrix interactions and are highlighted in italics.

GO and KEGG pathway analyses of pair-wise comparisons: PE apex versus vehicle apex. Genes altered in expression in the apex/apex pair-wise comparisons were also organized by KEGG pathway and GO. The relatively few number of genes that were significantly altered in this comparison (422 ≥1.5-fold, $P < 0.05$) were distributed into five KEGG pathways that each contained at least five genes, and only four pathways had a "▲" or a "▼" z-score >+2.0: arachidonic acid metabolism, ▼ +6.44; complement and coagulation cascades, ▲ +3.99; ECM-receptor interaction, ▲ +3.86; and TGF-β signaling pathway, ▲ +2.52.

Table 4. *Apex-selective gene expression*

Apex/Apex	Outflow/ Outflow	Gene Name	Gene ID
5.82▲	*4.8*▲	*suprabasin*	*Sbsn*
4▼	*6.32*▲	*regenerating islet-derived 3γ*	*Reg3 g*
3.7▲	7▲	myelin protein zero	Mpz
3.24▲	*2.6*▲	*similar to PIRA5*	*Lilrb3*
3.15▲	7.52▲	collagen, type VIII, α1	Col8a1
3.08▲	*2.64*▲	*natriuretic peptide precursor type B*	*Nppb*
2.84▼	*2.64*▲	*angiopoietin-like 4*	*Angptl4*
2.71▲	*2.47*▲	*hepcidin antimicrobial peptide*	*Hamp*
2.69▲	9.07▲	similar to Ig superfamily containing leu-rich repeat	LOC686539
2.61▲	11.45▲	similar to Coatomer γ-2 subunit (γ-2 coat protein)	RGD1566215
2.54▲	*<2.0*	*nuclear localized factor 2*	*Nlf2*
2.53▲	*<2.0*	*monoamine oxidase A*	*Maoa*
2.53▲	9.13▲	peptidase inhibitor 16	Pi16
2.52▲	12.59▲	α-2 μ globulin PGCL4	Obp3

List of genes with high PE apex/vehicle apex ratios not present in Table 2 (PEout/Vehout >15). PE apex/vehicle apex ratios are from Table 3; PE outflow/vehicle outflow ratios (<15) are from the complete gene list in Supplement 1. Genes with larger ratios in the apex/apex comparison relative to outflow/outflow AND/OR with different directions (▲ or ▼) are highlighted in italics.

The apex/apex ratios were also organized into GO terms. As with the data for the outflow/outflow comparison, lists were generated for the three primary terms, Biological Process, Cellular Component, and Molecular Function, and edited by z-score (Table 7). Because of the relatively few genes present in each secondary GO term, the list of genes was expanded in one secondary GO term for of the three primary terms in this table (growth, extracellular matrix, and structural molecule activity, respectively). The individual genes meeting the expression ratio threshold (≥1.5) with statistical significance are listed under the secondary GO terms. For the growth GO term, 14 genes were present in out of a total of 314 total genes annotated to this term. Thus, while the changes in the outflow tract are much more extensive, some changes in gene expression also occur in the apex region during PE.

DISCUSSION

Overview. The present studies examine changes in RV gene expression associated with chronic experimental pulmonary embolism in rats using DNA microarrays. Apex and outflow tract tissues were examined separately for several reasons. First, visual examination of whole hearts, staining of tissue-infiltrating leukocytes, and staining for extracellular matrix deposition indicate that the outflow tract is more severely damaged than the apex region (29, 31). Second, the outflow

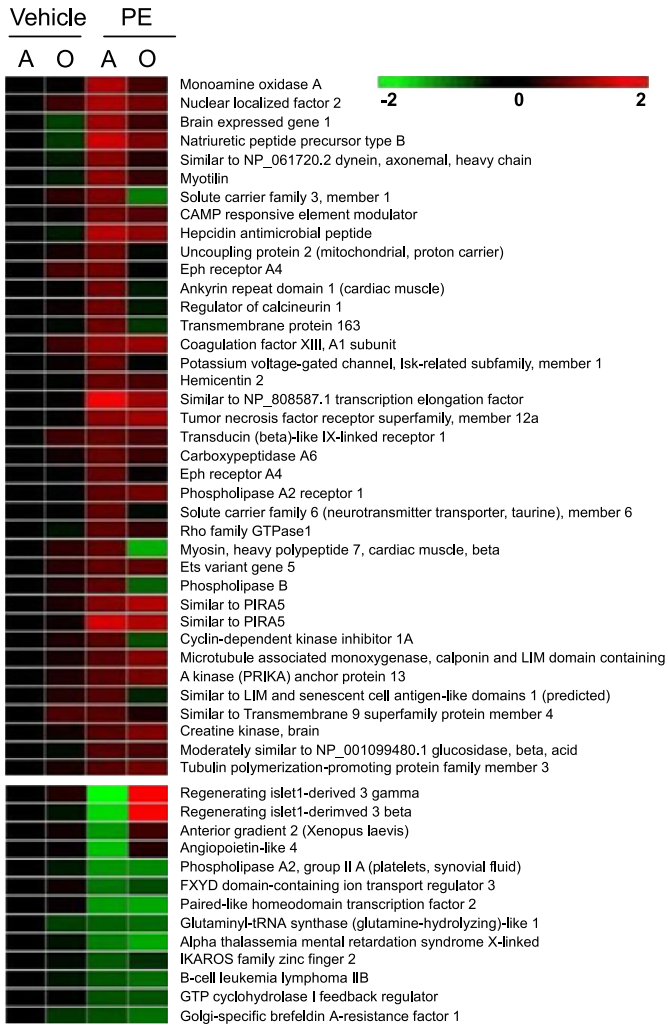

Fig. 4. HEAT map of genes with apex-selective expression based on pattern analysis of ANOVA results (1.5-fold expression threshold). *Lane 1*, vehicle apex (A); *lane 2*, vehicle outflow tract (O); *lane 3*, PE apex (A); *lane 4*, PE outflow tract (O). *Top*: genes identified with the pattern: control = 1, vehicle outflow tract <2, PE apex >2, PE outflow tract <2. *Bottom*: values set at control = 1, vehicle outflow >0.5, PE apex <0.5, PE outflow >0.5.

tract is relatively thin compared with the more muscular apex may therefore be more vulnerable to increased pulmonary artery resistance and elevated RV pressure (6, 11). Third, the outflow tract contracts later that the apex (6, 11). Since the outflow tract is thinner and contracts later than the apex, it would be expected to have greater stretch compared with the apex region in response to increased pulmonary vascular resistance. Finally, the outflow tract and apex have different embryologic origins, suggesting that even in maturity the transcriptional control mechanisms may differ in these two regions (6, 11).

The microarray assessment clearly indicated more alterations in outflow tract (over 8,000 genes) compared with the apex region (442 genes) following PE. Control (vehicle) outflow tract and control apex samples had few significant differences in gene expression. Thus, the differences observed with PE were not due to intrinsic regional variation in gene expression within the heart but were due to the effects of PE upon the RV tissue.

PE outflow versus vehicle outflow - inflammation. Table 8 summarizes chemokine data in the present study of chronic PE and compares them with the repertoire of chemokine genes expressed during 18 h PE from our previous study (36). Neutrophil accumulation is an early and transient response, peaking at 18 h and decreasing gradually over 1 wk (29). CXC chemokines are partially responsible for neutrophil recruitment during acute PE, since treatment of rats with antibodies against the CXC chemokine CINC-1 reduces RV inflammation and cardiac dysfunction (35). The role of monocytes in PE has yet to be determined. CD68+ monocytes accumulate in RV tissue during acute PE, but unlike the transient neutrophil accumulation, monocytes are present in RV tissues 6 wk after PE (29). We speculate that monocytes promote wound healing, tissue repair, and tissue remodeling. While nine CC-chemokine genes were elevated in the 18 h PE model, only three CC chemokines were expressed after 6 wk of PE, suggesting that these proteins participate in maintaining the recruitment of monocytes during chronic PE.

PE outflow versus vehicle outflow - metabolism. Our previous studies of 18 h PE showed decreasing expression of enzymes involved in fatty acid metabolism suggesting the conversion to the "fetal gene program" with metabolic preference for carbohydrates (36). The present studies indicate a very different profile is observed 6 wk after PE. The KEGG pathway analysis (Table 6) indicates large downward z-scores observed in all pathways of energy metabolism, including fatty acid, amino acid, and carbohydrate metabolism and overall mitochondrial processes, such as citric acid cycle and oxidative phosphorylation. The GO analysis (Table 5) also showed large decrease in metabolic process and organelle and catalytic activity that can be ascribed to decreases in expression of genes associated with metabolism and mitochondria. Histological evaluation suggests a possible explanation for the overall decrease in expression of metabolic pathways. The outflow tract from the 6 wk PE hearts contains reduced cardiac myocyte content, and the predominant cell types are fibroblasts, myofibroblasts, and monocytes (29). It has long been recognized that cardiac myocytes have a very high aerobic metabolic rate compared with other cell types (13, 23, 30). Thus, the decrease in expression of genes in metabolic pathways observed in the present studies may reflect a decrease in cardiac myocyte content and an increased proportion of cells with lower metabolic rates in the outflow tract of chronic PE hearts.

PE outflow versus vehicle outflow - extracellular matrix. Picrosirius red-stained collagen deposits were observed in RV outflow tissues and matrix metalloproteinases were activated in our previous study of chronic PE (29), which is consistent with the activation of wound healing pathways following RV damage. The current study identified altered expression of numerous genes involved in extracellular matrix deposition and remodeling as summarized in Tables 5 and 6. GO analysis showed large increases in the biological adhesion and extracellular matrix part. The genes included in this analysis are available in Supplement 6, middle and bottom panels. Furthermore, the second most highly induced gene in the chronic PE outflow tract (Table 2) was WISP2 (Wnt1-inducible signaling pathway protein 2, ▲ 70.64). WISP2 is a member of the CCN family of proteins (10). Several lines of evidence support a role for the CCN family of proteins in matrix remodeling. First, treatment of primary cardiac fibroblasts with WISP2 in vitro

Table 5. *Gene ontologies with significant z-scores in the PE outflow vs. vehicle outflow comparison*

Gene Ontologies	Total			Z-scores		
	List	▲	▼	Array	▲	▼
Biological Processes (13/23)						
●*Metabolic process*	*973*	*466*	*507*	*4,562*	*−5.72*	*3.84*
Biological regulation	836	515	321	3,967	2.61	−5.62
Regulation of biological process	757	473	284	3,611	2.68	−5.75
●*Developmental process*	554	373	181	2,303	*7.29*	*−4.04*
●*Multicellular organismal process*	544	367	177	2,322	*6.64*	*−4.52*
Establishment of localization	427	216	211	1,873	−0.75	2.10
Response to stimulus	421	268	153	1,802	4.22	−2.42
Positive regulation of biological process	291	208	83	1,211	5.98	−3.95
Negative regulation of biological process	237	154	83	1,101	2.16	−2.92
Immune system process	143	116	27	595	5.82	−4.61
●*Biological adhesion*	138	112	26	414	*9.65*	−2.59
Growth	83	65	18	314	4.82	−2.57
Cell killing	8	7	1	23	2.72	−0.90
Cellular Compartment (9/14)						
Cell	1,694	895	799	7,748	−5.85	4.43
Cell part	1,694	895	799	7,748	−5.85	4.43
●*Organelle*	1,024	474	550	4,697	*−6.53*	*6.28*
●*Organelle part*	514	215	299	2,355	*−5.30*	*5.37*
●*Extracellular region*	272	234	38	932	*12.82*	*−6.30*
Membrane-enclosed lumen	198	77	121	869	−3.14	4.21
●*Envelope*	165	30	135	425	*−3.30*	*15.50*
●*Extracellular region part*	156	137	19	490	*11.02*	*−4.59*
●*Extracellular matrix part*	39	34	5	84	*7.98*	*−1.22*
Molecular function (6/17)						
●*Catalytic activity*	798	360	438	3,199	*−0.60*	*9.97*
Molecular transducer activity	206	149	57	1,014	3.35	−4.47
Structural molecule activity	84	52	32	343	2.15	−0.11
●*Electron carrier activity*	47	14	33	148	*−0.79*	*5.35*
Antioxidant activity	14	7	7	36	1.49	2.04
Nutrient reservoir activity	1	1	0	1	2.77	−0.32

"Totals" indicates the number of individual genes (probe sets) in each column; "Array" indicates the number of genes annotated to an ontology that are imprinted on the array (rat 230 v2.0), while "List" indicates the number of genes in that ontology that were significantly altered in expression in the experiment. Symbols: "▲", genes within a gene ontology (GO) with PE2.0/vehicle ratio >1.0 (upregulated); "▼", genes within a GO with a fractional PE2.0/vehicle ratio (downregulated). Z-scores > +2.0 indicate that more genes in these ontologies were altered in expression than expected to occur at random. Z-scores < −2.0 indicate that fewer genes in these ontologies were altered in expression than expected to occur at random. Z-scores are given for up- and downregulated gene groups separately. Selected ontologies with large z-scores have been highlighted in italics.

led to fibroblast proliferation and increased collagen synthesis (4). Second, WISP2 is induced by load-stress (24) in bone in vivo and by shear stress in chondrocytes in vitro (21). Third, connective tissue growth factor (CTGF)/CCN2 is expressed in models of ischemic cardiac damage with fibrotic remodeling (7, 20). Lastly, treatment of cardiac myocytes in vitro with fibronectin, which is known to induce markers of the hypertrophic phenotype, induces expression of both CTGF and WISP2 (3).

Apex-selective expression. All of the genes significantly elevated in the apex tissue were elevated in the outflow tract samples of PE hearts. However, four genes showed greater change in PE apexes compared with PE outflows (Table 7). Two of these genes, angiopoeitin-like 4 and uncoupling protein 2 (UCP2), affect metabolism (2, 12, 26, 33). UCP2 also reduces the formation of reactive oxygen intermediates (2, 12) and protects against cell death (14) and ventricular hypertrophy (12). Ankrd1 is a stretch-responsive protein that is thought to be a negative transcriptional regulator (18, 37), possibly involved in cardiac adult-to-fetal reprogramming. Our previous study showed significant responses in Ankrd1 and fetal gene programming 18 h after PE (36), and Ankrd1 was selectively elevated in RV apexes during chronic PE. Thus, there are minimal transcriptional changes in the apex region of the RV in response to PE and those may relate to metabolism and stretch detection.

Summary

The present transcriptional data indicate that the RV outflow tract is subject to strong inflammatory responses, a reduction in metabolic gene expression, and upregulation of wound healing, extracellular matrix remodeling responses in chronic PE. These findings are consistent with previous histochemical observations, indicating a shift in cell types within the outflow tract tissue including the loss of cardiomyocyte cells with high energy requirements for contraction and replacement with cells involved in tissue remodeling and collagen deposition such as fibroblasts and monocytes. This response predicts a decrease in the contractile capacity of the outflow tract, but repair of acutely damaged outflow tracts via scar formation may convert a compromised and hemodynamically vulnerable outflow tract into a more stable, albeit noncontractile structure. In contrast with the outflow tract, there were minimal transcriptional changes in the apex region of the RV in response to PE.

Table 6. *Significant KEGG pathways in the PE2.0 outflow vs. vehicle outflow comparison*

KEGG Pathway	Totals				Z-scores	
	List	▲	▼	Array	▲	▼
Focal adhesion	50	37	13	141	4.72	−0.67
Regulation of actin cytoskeleton	42	29	13	153	2.18	−1.00
●*Oxidative phosphorylation*	33	0	33	71	*−3.33*	*9.72*
Cell communication	28	24	4	68	5.47	−1.35
Adipocytokine signaling pathway	27	12	15	62	1.46	3.38
●*ECM-receptor interaction*	27	24	3	50	*7.35*	*−1.13*
PPAR signaling pathway	27	11	16	62	1.08	3.79
Cell adhesion molecules (CAMs)	26	25	1	93	3.98	−3.10
●*Fatty acid metabolism*	25	5	20	36	0.13	8.63
●*Valine, leucine, and isoleucine degradation*	25	4	21	30	*0.03*	*10.42*
Hematopoietic cell lineage	20	16	4	63	2.91	−1.18
TGF-β signaling pathway	18	15	3	58	2.89	−1.42
●*Butanoate metabolism*	17	4	13	27	0.25	6.22
Glycolysis/Gluconeogenesis	17	6	11	42	0.22	3.19
Wnt signaling pathway	17	10	7	101	−0.99	−1.32
Complement and coagulation cascades	16	16	0	48	4.17	−2.45
●*Citrate cycle (TCA cycle)*	14	3	11	17	*0.55*	*7.12*
Carbon fixation	12	2	10	17	−0.17	6.34
Propanoate metabolism	11	0	11	20	−1.75	6.34
Fructose and mannose metabolism	10	2	8	27	−0.89	3.13
Lysine degradation	9	3	6	18	0.44	3.05
Pyruvate metabolism	9	2	7	24	−0.70	2.87
Phenylalanine metabolism	8	3	5	13	1.06	3.19
Alanine and aspartate metabolism	7	2	5	18	−0.26	2.30
β-Alanine metabolism	7	2	5	17	−0.17	2.45
Caprolactam degradation	5	0	5	8	−1.10	4.68
Glycan structures - degradation	5	4	1	11	2.28	−0.20
Reductive carboxylate cycle (CO2 fixation)	5	1	4	7	0.09	3.92
Synthesis and degradation of ketone bodies	5	2	3	5	1.78	3.52

Header terms are defined in Table 6 for GO. The list of pathways is stratified by descending number of genes present in each "list".

ACKNOWLEDGMENTS

We thank the members of the Cannon Research Center Microarray Core Facility for performing the GeneChip hybridizations: Dr. Nury Steuerwald, core Director; Judy Vachris-Benson; and Kris Bennett. We also thank Kris Bennett for conducting the quantitative real-time PCR.

GRANTS

This work was supported in part by a grant from the Education and Research Committee of the Charlotte-Mecklenburg Health Services Foundation to J. Zagorski.

REFERENCES

1. **Begieneman MP, van de Goot FR, van der Bilt IA, Vonk Noordegraaf A, Spreeuwenberg MD, Paulus WJ, van Hinsbergh VW, Visser FC, Niessen HW.** Pulmonary embolism causes endomyocarditis in the human heart. *Heart* 94: 450–456, 2008.
2. **Bo H, Jiang N, Ma G, Qu J, Zhang G, Cao D, Wen L, Liu S, Ji LL, Zhang Y.** Regulation of mitochondrial uncoupling respiration during exercise in rat heart: role of reactive oxygen species (ROS) and uncoupling protein 2. *Free Radic Biol Med* 44: 1373–1381, 2008.
3. **Chen H, Huang XN, Stewart AF, Sepulveda JL.** Gene expression changes associated with fibronectin-induced cardiac myocyte hypertrophy. *Physiol Genomics* 18: 273–283, 2004.
4. **Colston JT, de la Rosa SD, Koehler M, Gonzales K, Mestril R, Freeman GL, Bailey SR, Chandrasekar B.** Wnt-induced secreted protein-1 is a prohypertrophic and profibrotic growth factor. *Am J Physiol Heart Circ Physiol* 293: H1839–H1846, 2007.
5. **Courtney DM, Watts JA, Kline JA.** End tidal CO_2 is reduced during hypotension and cardiac arrest in a rat model of massive pulmonary embolism. *Resuscitation* 53: 83–91, 2002.
6. **Dell'Italia LJ.** The right ventricle: anatomy, physiology, and clinical importance. *Curr Probl Cardiol* 16: 653–720, 1991.
7. **Gabrielsen A, Lawler PR, Yongzhong W, Steinbruchel D, Blagoja D, Paulsson-Berne G, Kastrup J, Hansson GK.** Gene expression signals involved in ischemic injury, extracellular matrix composition and fibrosis defined by global mRNA profiling of the human left ventricular myocardium. *J Mol Cell Cardiol* 42: 870–883, 2007.
8. **Goldhaber SZ, Elliott CG.** Acute pulmonary embolism: part I: epidemiology, pathophysiology, and diagnosis. *Circulation* 108: 2726–2729, 2003.
9. **Goldhaber SZ, Elliott CG.** Acute pulmonary embolism: part II: risk stratification, treatment, and prevention. *Circulation* 108: 2834–2838, 2003.
10. **Gray MR, Malmquist JA, Sullivan M, Blea M, Castellot JJ Jr.** CCN5 Expression in mammals. II. Adult rodent tissues. *J Cell Commun Signal* 1: 145–158, 2007.
11. **Haddad F, Hunt SA, Rosenthal DN, Murphy DJ.** Right ventricular function in cardiovascular disease, part I: anatomy, physiology, aging, and functional assessment of the right ventricle. *Circulation* 117: 1436–1448, 2008.
12. **Hang T, Jiang S, Wang C, Xie D, Ren H, Zhuge H.** Apoptosis and expression of uncoupling protein-2 in pressure overload-induced left ventricular hypertrophy. *Acta Cardiol* 62: 461–465, 2007.
13. **Harris DA, Das AM.** Control of mitochondrial ATP synthesis in the heart. *Biochem J* 280: 561–573, 1991.
14. **Hoerter J, Gonzalez-Barroso MD, Couplan E, Mateo P, Gelly C, Cassard-Doulcier AM, Diolez P, Bouillaud F.** Mitochondrial uncoupling protein 1 expressed in the heart of transgenic mice protects against ischemic-reperfusion damage. *Circulation* 110: 528–533, 2004.
15. **Iwadate K, Doi M, Tanno K, Katsumura S, Ito H, Sato K, Yonemura I, Ito Y.** Right ventricular damage due to pulmonary embolism: examination of the number of infiltrating macrophages. *Forensic Sci Int* 134: 147–153, 2003.
16. **Iwadate K, Tanno K, Doi M, Takatori T, Ito Y.** Two cases of right ventricular ischemic injury due to massive pulmonary embolism. *Forensic Sci Int* 116: 189–195, 2001.
17. **Jones AE, Watts JA, Debelak JP, Thornton LR, Younger JG, Kline JA.** Inhibition of prostaglandin synthesis during polystyrene microsphere-

Table 7. *Significant GOs in the PE apex vs. vehicle apex comparison*

GOs	Totals				Z-scores	
	List	▲	▼	Array	▲	▼
Biological Processes (6/23)						
Multicellular organismal process	73	63	10	2,322	4.02	0.79
Developmental process	65	57	8	2,303	2.98	−0.01
Response to stimulus	53	46	7	1,802	2.81	0.32
Positive regulation of biological process	39	34	5	1,211	2.93	0.41
Biological adhesion	21	20	1	414	4.81	−0.38
Growth	14	14	0	314	3.66	−1.07
▲ 1.98, Bone morphogenetic protein 6						
▲ 2.66, Connective tissue growth factor						
▲ 1.55, FXYD domain-containing ion transport regulator 2						
▲ 1.75, Growth-associated protein 43						
▲ 1.54, Heparin-binding EGF-like growth factor						
▲ 2.24, Immunoglobulin superfamily, member 10						
▲ 20.44, Natriuretic peptide precursor type A						
▲ 1.96, Ninjurin 2						
▲ 2.15, Prostaglandin-endoperoxide synthase 2						
▲ 1.63, SRY-box containing gene 10						
▲ 1.76, TGF-β2						
▲ 1.80, TGF-β3						
▲ 1.59, Versican						
▲ 6.41, WNT1-inducible signaling pathway protein 2						
Cellular compartment (3/14)						
Extracellular region	66	61	5	932	11.92	1.23
Extracellular region part	36	34	2	490	9.09	0.35
Extracellular matrix part	10	10	0	84	7.17	−0.52
▲ 1.63, Collagen, type I, α1						
▲ 1.64, Collagen, type I, α2						
▲ 1.71, Collagen, type XII, α1						
▲ 1.61, Collagen, type XVIII, α1						
▲ 1.99, Fibrillin 1						
▲ 1.70, Fibulin 1						
▲ 1.76, Hemicentin 2						
▲ 2.00, Microfibrillar-associated protein 5						
▲ 1.77, K^+ volt-gated channel, Isk-related, member 1						
▲ 1.54, Tissue inhibitor of metalloproteinase 2						
Molecular function (2/17)						
Structural molecule activity	14	14	0	343	3.54	−1.06
▲ 1.63, Collagen, type I, α1						
▲ 1.64, Collagen, type I, α2						
▲ 1.71, Collagen, type XII, α1						
▲ 1.64, Collagen, type XIV, α1						
▲ 1.61, Collagen, type XVIII, α1						
▲ 1.78, Elastin						
▲ 1.99, Fibrillin 1						
▲ 1.79, Myelin basic protein						
▲ 3.71, Myelin protein zero						
▲ 1.69, Myosin, heavy polypeptide 7, cardiac-β						
▲ 1.53, Proteolipid protein (myelin) 1						
▲ 2.61, Similar to Coatomer γ-2 subunit						
▲ 7.14, thrombospondin 4						
▲ 1.51, Transmembrane protein 178						
nutrient reservoir activity	1	1	0	1	7.66	−0.06

induced pulmonary embolism in the rat. *Am J Physiol Lung Cell Mol Physiol* 284: L1072–L1081, 2003.

18. **Kemp TJ, Sadusky TJ, Saltisi F, Carey N, Moss J, Yang SY, Sassoon DA, Goldspink G, Coulton GR.** Identification of Ankrd2, a novel skeletal muscle gene coding for a stretch-responsive ankyrin-repeat protein. *Genomics* 66: 229–241, 2000.
19. **Kline JA, Hernandez-Nino J, Rose GA, Norton HJ, Camargo CA Jr.** Surrogate markers for adverse outcomes in normotensive patients with pulmonary embolism. *Crit Care Med* 34: 2773–2780, 2006.
20. **Koitabashi N, Arai M, Kogure S, Niwano K, Watanabe A, Aoki Y, Maeno T, Nishida T, Kubota S, Takigawa M, Kurabayashi M.** Increased connective tissue growth factor relative to brain natriuretic peptide as a determinant of myocardial fibrosis. *Hypertension* 49: 1120–1127, 2007.
21. **Lee MS, Sun MT, Pang ST, Ueng SW, Chen SC, Hwang TL, Wang TH.** Evaluation of differentially expressed genes by shear stress in human osteoarthritic chondrocytes in vitro. *Chang Gung Med J* 32: 42–50, 2009.
22. **McConnell MV, Solomon SD, Rayan ME, Come PC, Goldhaber SZ, Lee RT.** Regional right ventricular dysfunction detected by echocardiography in acute pulmonary embolism. *Am J Cardiol* 78: 469–473, 1996.
23. **Neely JR, Morgan HE.** Relationship between carbohydrate and lipid metabolism and the energy balance of heart muscle. *Ann Rev Physiol* 36: 413–459, 1974.
24. **Robinson JA, Chatterjee-Kishore M, Yaworsky PJ, Cullen DM, Zhao W, Li C, Kharode Y, Sauter L, Babij P, Brown EL, Hill AA, Akhter MP, Johnson ML, Recker RR, Komm BS, Bex FJ.** Wnt/beta-catenin signaling is a normal physiological response to mechanical loading in bone. *J Biol Chem* 281: 31720–31728, 2006.

Table 8. *Chemokine expression in RV tissue during acute and chronic PE*

Chemokine	RV, Acute PE	Outflow Tract, Chronic PE
CCL2/MCP-1	35.81▲	2.37▲
CCL3/MIP1α	11.62▲	<2
CCL4/MIP1β	6.28▲	<2
CCL6/C10	2.0▲	<2
CCL7/MCP3	52.27▲	<2
CCL9/MIP1γ	3.95▲	<2
CCL17/TARC	3.59▲	<2
CCL19/MIP3β	<1.5	3.53▲
CCL20/MIP3α	8.98▲	<2
CCL21b/6Ckine	<1.5	5.85▲
CCL27/ESkine	9.15▲	<2
CXCL1/CINC-1	26.88▲	2.34▲
CXCL2/CINC-2	18.38▲	<2
CXCL9/MIG	1.65▲	<2
CXCL10/IP-10	2.47▲	<2
CXCL11/ITAC	<1.5	5.86▼
CXC12/SDF-1	3.61▼	5.34▲
CXCL13/BLC	<1.5	6.66▲
CXCL16/SRPSOX	2.07▲	3.74▲
XCL1/LTN	2.21▼	<2

Data for "acute PE" have been taken from Zagorski et al. (60). Data for "outflow tract" are from Supplement 1, PE outflow tract/vehicle outflow tract ratios. RV, right ventricle.

25. **Schoepf UJ, Kucher N, Kipfmueller F, Quiroz R, Costello P, Goldhaber SZ.** Right ventricular enlargement on chest computed tomography: a predictor of early death in acute pulmonary embolism. *Circulation* 110: 3276–3280, 2004.
26. **Staiger H, Haas C, Machann J, Werner R, Weisser M, Schick F, Machicao F, Stefan N, Fritsche A, Haring HU.** Muscle-derived angiopoietin-like protein 4 is induced by fatty acids via peroxisome proliferator-activated receptor (PPAR)-delta and is of metabolic relevance in humans. *Diabetes* 58: 579–589, 2009.
27. **Stevinson BG, Hernandez-Nino J, Rose G, Kline JA.** Echocardiographic and functional cardiopulmonary problems six months after first-time pulmonary embolism in previously healthy patients. *Eur Heart J* 28: 2517–2524, 2007.
28. **Tapson VF.** Acute pulmonary embolism. *N Engl J Med* 358: 1037–1052, 2008.
29. **Watts JA, Gellar MA, Obraztsova M, Kline JA, Zagorski J.** Role of inflammation in right ventricular damage and repair following experimental pulmonary embolism in rats. *Int J Exp Path* 89: 389–399, 2008.
30. **Watts JA, Kline JA.** Bench-to-Bedside: The role of mitochondrial medicine in the pathogenesis and treatment of cellular injury. *Acad Emerg Med* 10: 1–10, 2003.
31. **Watts JA, Zagorski J, Gellar MA, Stevinson BG, Kline JA.** Cardiac inflammation contributes to right ventricular dysfunction following experimental pulmonary embolism in rats. *J Mol Cell Cardiol* 41: 296–307, 2006.
32. **Wood KE.** Major pulmonary embolism: review of a pathophysiologic approach to the golden hour of hemodynamically significant pulmonary embolism. *Chest* 121: 877–905, 2002.
33. **Xu A, Lam MC, Chan KW, Wang Y, Zhang J, Hoo RL, Xu JY, Chen B, Chow WS, Tso AW, Lam KS.** Angiopoietin-like protein 4 decreases blood glucose and improves glucose tolerance but induces hyperlipidemia and hepatic steatosis in mice. *Proc Natl Acad Sci USA* 102: 6086–6091, 2005.
34. **Zagorski J, Debelak J, Gellar M, Watts JA, Kline JA.** Chemokines accumulate in the lungs of rats with severe pulmonary embolism induced by polystyrene microspheres. *J Immunol* 171: 5529–5536, 2003.
35. **Zagorski J, Gellar MA, Obraztsova M, Kline JA, Watts JA.** Inhibition of CINC-1 Decreases Right Ventricular Damage Caused by Experimental Pulmonary Embolism in Rats. *J Immunol* 179: 7820–7826, 2007.
36. **Zagorski J, Sanapareddy N, Gellar MA, Kline JA, Watts JA.** Transcriptional profile of right ventricular tissue during acute pulmonary embolism in rats. *Physiol Genomics* 34: 101–111, 2008.
37. **Zolk O, Frohme M, Maurer A, Kluxen FW, Hentsch B, Zubakov D, Hoheisel JD, Zucker IH, Pepe S, Eschenhagen T.** Cardiac ankyrin repeat protein, a negative regulator of cardiac gene expression, is augmented in human heart failure. *Biochem Biophys Res Commun* 293: 1377–1382, 2002.